

# On the Imaging Mechanism of Ferroelectric Domains in Scanning Force Microscopy

A. Gruverman\*

*Department of Materials Science and Engineering, North Carolina State University,  
Raleigh, North Carolina 27695*

H. Tokumoto

*Joint Research Center for Atom Technology, National Institute for Advanced  
Interdisciplinary Research, Higashi 1-1-4, Tsukuba, Ibaraki 305, Japan*

Received November 9, 2000

## ABSTRACT

Scanning force microscopy (SFM) studies of the domain structure in ferroelectric thin films on a nonmetal substrate allowed direct assessment of the electrostatic mechanism contribution to the domain contrast in the SFM contact mode. It has been shown that the polarization charges of the ferroelectric film are effectively compensated. This result suggests secondary effect of the electrostatic tip-sample interaction on domain imaging mechanism in ferroelectric thin films in contact SFM compared to the major contribution of the piezoelectric effect.

Scanning force microscopy (SFM) has become a powerful tool for the characterization of ferroelectric materials, providing crucial information on their dielectric properties at the nanoscale level. A particular attraction of SFM is that it allows nondestructive nanoscale visualization and precise control of domain structures in ferroelectric thin films,<sup>1–3</sup> an accomplishment which looked very difficult several years ago. Direct imaging of ferroelectric domains by means of SFM has proved to be particularly effective in elucidating the microscopic mechanisms of polarization reversal and degradation effects such as fatigue and retention loss in ferroelectric films.<sup>2–12</sup> Most of the SFM studies of ferroelectric domains in thin films are based on the application of a modulation voltage to a probing tip in contact with the film surface. It is assumed that the applied voltage generates a local film surface vibration due to the converse piezoelectric effect (that is why this method has been often called piezoresponse SFM).<sup>1–10</sup> The phase and the amplitude of the vibration signal detected by the lock-in technique provide information about the polarization direction and the value of the piezoelectric coefficient, respectively. However, there is an alternative view on the mechanism of domain imaging in contact SFM; namely, it is attributed to the electrostatic tip-sample interaction due to the presence of surface polarization charges in the ferroelectric sample.<sup>11–15</sup> From the physical point of view both effects should take place during domain imaging. However, it is argued that their

contribution to the measured signal is quantitatively different depending on the sample properties and experimental conditions. It has been shown that the piezoresponse and electrostatic methods produce almost identical images of the poled domain patterns in thin films.<sup>16</sup> If somehow one of the effects would be suppressed, then the contribution of the other could be directly estimated. In the present paper, we performed domain imaging in  $\text{PbZr}_{0.20}\text{Ti}_{0.80}\text{O}_3$  (PZT) films without the bottom electrode, which has allowed us to exclude the contribution of the piezoelectric effect to the domain image. The obtained results, which showed that the polarization charges are effectively compensated, led us to conclude that in contact SFM the piezoelectric effect plays a dominant role in ferroelectric domain imaging mechanism in film/electrode heterostructures.

Experiments were performed by means of a commercial force microscope (Seiko Instruments SPI 3700) using 210 nm thick PZT films deposited by laser ablation at 600 °C and 100 mTorr oxygen pressure on a  $\text{LaAlO}_3$  substrate (LAO). The thickness of the LAO substrate, which was mounted on the grounded sample holder, is about 500  $\mu\text{m}$ . Domain images have been acquired by applying an ac modulation voltage with an amplitude of 10 V and a frequency of 10 kHz. The modulation voltage was applied to a standard Au-coated silicon nitride cantilever. The microscope was operated in a contact mode (repulsive force regime).

Figure 1a shows a topographic image of the PZT film. A domain structure consisting of a and c domains (with in-

\* Corresponding author. E-mail: Alexei\_Gruverman@ncsu.edu.

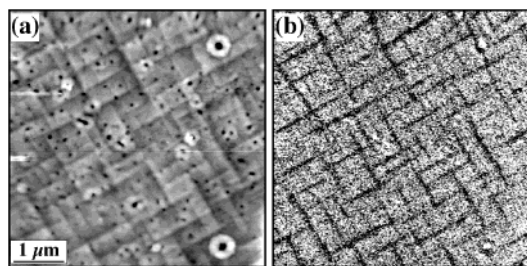


**Figure 1.** (a) Topographic image of  $\text{PbZr}_{0.20}\text{Ti}_{0.80}\text{O}_3$  film on a  $\text{LaAlO}_3$  substrate showing a rectangular a-c domain pattern, visible due to the tilting of the surfaces of c and a domains with respect to each other. (b) Electrostatic domain image obtained as a result of the ac voltage modulation.

plane and out-of-plane polarization, respectively) that develops in epitaxial ferroelectric thin films as a result of strain energy relaxation<sup>17</sup> can be clearly seen. The rectangular a-c domain pattern appears in the topographic image due to the tilting of the surfaces of c and a domains with respect to each other.<sup>2,18</sup> Twinning between a and c domains led to the height variations in the range of 1.5–3.5 nm. A domain image obtained as a result of the voltage modulation is shown in Figure 1b. Since the applied voltage drops across the LAO substrate and therefore no piezoelectric effect is induced, this domain image could be attributed only to the electrostatic interaction between the biased probing tip and surface charges. (It is assumed that, even in the contact mode, there is a small gap between the tip and the sample surface and therefore they are not at the same potential.) The electrostatic mechanism of domain imaging in contact SFM has been described in detail by Terris et al.<sup>19</sup> and Hong et al.<sup>13</sup> It has been suggested that when an ac modulation voltage  $V = V_{\text{ac}} \cos(\omega t)$  is applied to the probing tip, the  $w$  component of the electrostatic tip-sample interaction force can be written as

$$F_e(w) = (\sigma_b C / 2\epsilon_0) V_{\text{ac}} \cos(\omega t) \quad (1)$$

where  $\sigma_b$  is the bounded surface charge density equal to spontaneous polarization,  $\epsilon_0$  is the dielectric constant, and  $C$  is the tip-sample capacitance. The difference in electrostatic forces measured above the charged surface of c domains and the surface of a domains, which do not have surface polarization charges, provides the domain contrast in Figure 1b. Note that surface defects seen in Figure 1a have not been imaged in Figure 1b, suggesting that topographic features have little effect on domain image.

For quantitative estimation of the bounded surface charge density, we will use a method suggested by Hong et al.<sup>13</sup> The surface charge density can be estimated by measuring a dc tip bias at which the  $w$  component of the electrostatic force vanishes.<sup>13</sup> When a dc bias  $V_{\text{dc}}$  is applied to the tip during scanning along with the ac voltage, an additional term appears in the  $w$  component of the electrostatic force:

$$F_e(w) = \left( \frac{\partial C}{\partial z} V_{\text{dc}} + \sigma_b C / 2\epsilon_0 \right) V_{\text{ac}} \cos(\omega t) \quad (2)$$

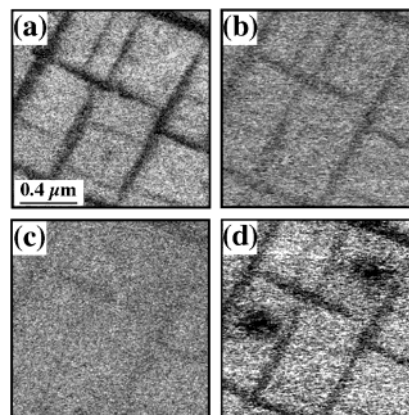


**Figure 2.** Electrostatic domain images obtained at different dc biases: (a)  $V_{\text{dc}} = 0$  V; (b)  $V_{\text{dc}} = 0.2$  V; (c)  $V_{\text{dc}} = 0.5$  V. (d) Electrostatic domain image obtained at a zero dc bias. Two dark circular spots seen in this image appeared after an ac voltage of 10 V was applied to these sites for about 10 min by the fixed probing tip.

where  $z$  is a tip-sample distance. A charge, induced in the gold layer of the tip by the electrostatic field of the sample and the applied voltage, interacts with the bound charges of c domains. By adjusting the dc bias, it is possible to compensate this induced charge and therefore to suppress the electrostatic interaction. As a result, the contrast between a and c domains will disappear. Figure 2 shows the results obtained using this method. The original domain contrast observed in Figure 2a at the zero dc bias fades under the dc bias of 0.2 V (Figure 2b) applied during scanning and disappears at 0.5 V (Figure 2c).

Assuming that for contact SFM a parallel plate capacitor model can be used, it is possible to write  $(\partial C / \partial z) / C \cong 1/z$ . For  $V_{\text{dc}} = 0.5$  V and  $z = 1$  nm we obtained  $\sigma_b = 0.8 \mu\text{C}/\text{cm}^2$ . This value is almost 2 orders of magnitude lower than the previously reported value of the spontaneous polarization of about  $50 \mu\text{C}/\text{cm}^2$  in PZT films.<sup>20</sup> Even from this oversimplified model it can be understood that the polarization charges of the PZT film are effectively compensated by accumulation of free charge carriers from the environment on the film surface. Application of the external dc or ac voltage for sufficiently long time could change the surface charge distribution and, as a result, alter the electrostatic image of the domain pattern. This effect is illustrated in Figure 2d. Application of the ac voltage of 10 V to two sites on the film surface for about 10 min through the fixed SFM tip resulted in appearance of two dark circular spots in Figure 2d due to the changed distribution of surface charges. Another reason for the small value of  $\sigma_b$  is the contamination layer, which is always present at the sample surface under ambient conditions. This layer could reduce the electrostatic interaction between the tip and the sample. The vibration amplitude signal measured in the present experiment was less than  $100 \mu\text{V}$ , compared to  $500 \mu\text{V}$  typically measured during piezoresponse measurements of ferroelectric thin films.<sup>3</sup> Therefore, we concluded that, in the SFM contact mode, under typical experimental conditions used for domain observation,<sup>2–10</sup> the ferroelectric domain imaging mechanism in film/electrode heterostructures is not due to the electro-

static interaction but is mainly due to the piezoelectric effect. However, the situation might be different in ferroelectric crystals with the low value of the piezoelectric coefficient.<sup>14</sup> In this case, given that the field generated by the SFM tip is highly inhomogeneous, i.e., it is very strong at the film surface but quickly decreases with distance in the film polar direction which leads to the vanishing of the piezoresponse, the contribution to domain contrast from piezoelectric and electrostatic effects could be comparable.

In conclusion, SFM imaging of the a–c domain pattern in PZT films on the nonmetal substrate allowed direct assessment of the electrostatic signal contribution to the domain image in the contact mode. The obtained results showed that in ambient conditions the polarization charges are effectively compensated by free charge carriers from the environment and cannot significantly affect the domain contrast. It is, therefore, concluded that in the SFM contact mode the main imaging mechanism of ferroelectric domains in thin film/electrode heterostructures is the piezoelectric effect.

## References

- (1) Franke, K.; Besold, J.; Haessler, W.; Seegebarth, C. *Surf. Sci. Lett.* **1994**, 302, L283.
- (2) Gruverman, A.; Auciello, O.; Tokumoto, H. *Integrated Ferroelectrics* **1998**, 19, 49.
- (3) Gruverman, A.; Auciello, O.; Tokumoto, H. *Annu. Rev. Mater. Sci.* **1998**, 28, 101.
- (4) Hidaka, T.; Maruyama, T.; Sakai, I.; Saitoh, M.; Wills, L. A.; Hiskes, R.; Dicarolis, S. A.; Amano, J. *Integrated Ferroelectrics* **1997**, 17, 319.
- (5) Yoo, I. K.; Kim, B. M.; Kim, D. S.; Park, S. J. *Mater. Res. Soc. Symp. Proc.* **1998**, 493, 299.
- (6) Eng, L. *Nanotechnology* **1999**, 10, 405.
- (7) Ganpule, C. S.; Stanishevsky, A.; Su, Q.; Aggarwal, S.; Melngailis, J.; Williams, E.; Ramesh, R. *Appl. Phys. Lett.* **1999**, 75, 409.
- (8) Colla, E. L.; Hong, S.; Taylor, D. V.; Tagantsev, A. K.; Setter, N. *Appl. Phys. Lett.* **1998**, 72, 2763.
- (9) Hong, S.; Colla, E. L.; Kim, E.; Taylor, D. V.; Tagantsev, A. K.; Murali, P.; No, K.; Setter, N. *J. Appl. Phys.* **1999**, 86, 607.
- (10) Harnagea, C.; Pignolet, A.; Alexe, M.; Satyalakshmi, K. M.; Hesse, D.; Gösele, U. *Jpn. J. Appl. Phys.* **1999**, 38, part 2, L1255.
- (11) Hong, J. W.; Jo, W.; Kim, D. C.; Cho, S. M.; Nam, H. J.; Lee, H. M.; Bu, J. U. *Appl. Phys. Lett.* **1999**, 75, 3183.
- (12) Jo, W.; Kim, D. C.; Hong, J. W. *Appl. Phys. Lett.* **2000**, 76, 390.
- (13) Hong, J. W.; Noh, K. H.; Park, S.-I.; Kwun, S. I.; Khim, Z. G. *Phys. Rev. B* **1998**, 58, 5078.
- (14) Likodimos, V.; Orlik, X. K.; Pardi, L.; Labardi, M.; Allegrini, M. *J. Appl. Phys.* **2000**, 87, 443.
- (15) Luo, E. Z.; Xie, Z.; Xu, J. B.; Wilso, I. H.; Zhao, L. H. *Phys. Rev. B* **2000**, 61, 203.
- (16) Chen, X. Q.; Yamada, H.; Horiuchi, T.; Matsushige, K.; Watanabe, S.; Kawai, M.; Weiss, P. S. *J. Vac. Sci. Technol.* **1999**, B17, 1930.
- (17) Pompe, W.; Gong, X.; Suo, Z.; Speck, J. S. *J. Appl. Phys.* **1993**, 74, 6012.
- (18) Hamazaki, S.-I.; Shimizu, F.; Kojima, S.; Takashige, M. *J. Phys. Soc. Jpn.* **1995**, 64, 3660.
- (19) Terris, B. D.; Stern, J. E.; Rugar, D.; Mamin, H. J. *Phys. Rev. Lett.* **1989**, 63, 2669.
- (20) Foster, C. M.; Bai, G.-R.; Csencsits, R.; Vetrone, J.; Jammy, R.; Wills, L. A.; Carr, E.; Jun Amano J. *Appl. Phys.* **1997**, 81, 2349.

NL005522R